Andreev reflections at metal/superconductor point contacts: Measurement and analysis

G. J. Strijkers, Y. Ji, F. Y. Yang, and C. L. Chien
Department of Physics and Astronomy, The Johns Hopkins University, Baltimore, Maryland 21218

J. M. Byers
Naval Research Laboratory, Washington, DC 20375

(Received 19 September 2000; revised manuscript received 20 November 2000; published 15 February 2001)

We present point-contact Andreev reflection measurements of X/Nb contacts, where $X=$ Ni, Co, Fe, and Cu. Experimental conductance-voltage curves were analyzed with the Blonder-Tinkham-Klapwijk theory [Phys. Rev. B **25**, 4515 (1982)], extended to include the polarization P of the metal and proximity effects. For Ni, Co, and Fe the conductance-voltage curves can be well described by the model with P and Z as the fitting parameters, where Z is a dimensionless barrier strength included in the model to describe elastic scattering at a nonideal metal/superconductor interface. The polarization for Fe, Co, and Ni depends on the magnitude of Z. The value of the intrinsic P can be obtained by extrapolation to $Z=0$ (perfectly transparent interface). For Cu, the conductance-voltage curves show a dip at the position of the Nb superconducting gap, due to proximity effects, which reduce the effective gap value for the normal to supercurrent conversion at the Cu/Nb interface, while leaving the gap for quasiparticle transport essentially unchanged. In addition, an overall decrease of the gap is observed when the size of the point contact approaches the superconducting coherence length in Nb. We have included these effects in our model and obtained very good agreement between experimental data and model calculations.

DOI: 10.1103/PhysRevB.63.104510 PACS number(s): 74.80.Fp, 75.30.−m, 75.70.−i, 74.50.+r

I. INTRODUCTION

Recently, there is a renewed experimental and theoretical interest in metal/super-conductor junctions, largely driven by the ability to measure the spin polarization P of the conduction electrons in a metal with the so-called point-contact Andreev reflection (PCAR) method.[1–3] The rapid development of new magnetoelectronic devices in recent years stimulates the search for materials with a high spin polarization as the performance of such devices depends critically on a substantial spin polarization.[4,5] A reliable method for the determination of P for newly developed materials is therefore of prime importance.

The spin polarization of a metal is usually defined as $P_n=(n^{\uparrow}-n^{\downarrow})/(n^{\uparrow}+n^{\downarrow})$, where $n^{\uparrow}$ and $n^{\downarrow}$ are the charge densities at the Fermi energy of the majority band and the minority band, respectively. However, in the measurements of spin polarization by PCAR or tunneling, one measures $P=(I^{\uparrow}-I^{\downarrow})/(I^{\uparrow}+I^{\downarrow})$, the imbalance in the currents of the majority and minority carriers.[3] We will use this definition of P, which is relevant to spin polarization measured by PCAR, in the remainder of this paper. The value of P is not necessarily the same as that of P_n. Under certain conditions, such as when the Fermi velocities of all the spin currents are the same, $P=P_n$.[6] Note that, although $I^{\uparrow}$ can be either larger or smaller than $I^{\downarrow}$, with PCAR we can only measure the absolute value of the spin polarization $|P|$.

Apart from PCAR, there are only a few other methods with which one can determine P. The most widely used method, so far, uses a superconducting tunnel junction, consisting of a superconductor/insulator/ferromagnet stack of layers.[7–9] The value of P can be determined by exploiting the characteristics of the density of states of the superconductor in a magnetic field. There are however a number of drawbacks to this method. Tunneling occurs only from within a few monolayers at the interfaces between the metal electrodes and the insulating barrier layer.[10] The spin polarization of these few interfacial layers can be substantially different from that of the bulk. Furthermore, the fabrication of a pinhole-free insulating barrier layer with a thickness of about 1 nm proves to be extremely difficult. The characteristics of the barrier material must also be taken into account in the determination of P via the tunneling matrix elements. Indeed, a wide range of values have been reported for the spin polarization of Ni, Co, Fe, and some of their alloys, when using Al_2O_3, AlN, and MgO as barriers.[8]

In contrast, PCAR does not suffer from these drawbacks as it does not rely on the preparation of a thin insulating barrier layer and it probes the polarization not merely at a few monolayers at the interface but on the lengthscale of the electron mean free path in the metal. Furthermore, PCAR is very well suited for the measurement of the spin polarization of new materials, for which the fabrication of high quality tunnel junctions is often a formidable challenge.

Nevertheless, while the principle of PCAR in ideal situations appears to be simple, employing the technique in real experimental conditions is nontrivial. Without suitable analysis, the as-obtained PCAR results can lead to exaggerated values of P. In this paper, we will present PCAR measurements and model calculations, providing a methodology through which the PCAR results can be reliably interpreted and the value of P extracted. Ferromagnetic Ni, Co, Fe, and their alloys are the most important materials to date with substantial spin polarization. However, the reported values of spin polarization of even these well-known ferromagnets vary greatly. We will demonstrate that the spin polarization of Ni, Co, and Fe can be accurately determined using PCAR. For nonmagnetic metals, the spin polarization is expected to

 ©2001 The American Physical Society

be zero. Strong proximity effects must be taken in account, however, in order to extract the spin polarization from the PCAR measurements, as demonstrated in the case of Cu.

The outline of this paper is as follows. In Sec. II, we will discuss the model used to fit the experimental results of Sec. IV. After a brief description of the experimental procedure (Sec. III), we will present the Andreev reflection measurements for the magnetic materials Ni, Co, and Fe, and for nonmagnetic Cu in Sec. IV. These results will be analyzed and discussed using the model of Sec. II. Finally, we will summarize and conclude in Sec. V.

II. MODEL

When a bias voltage V is applied across a clean nonmagnetic-metal/superconductor point contact, there are several mechanisms for the current to enter the superconductor. At voltages higher than the superconducting gap Δ, electrons can pass from the metal into the superconductor as quasielectrons or holes, which relax into the Cooper-pair condensate over the charge relaxation distance. However, for voltages lower than the superconducting gap Δ, there are no available quasiparticle states in the superconductor. Instead, current is converted directly into a supercurrent of Cooper pairs, consisting of two electrons of charge e with opposite spin. This is accomplished by the reflection of a hole back into the metal, a process first described by Andreev.[11] Thus for Andreev reflection $2e$ is transferred across the interface, effectively doubling the conductance as compared to the normal-state conductance, i.e., $G(0)/G_n=2$, where $G(0)$ is the conductance at zero bias and G_n the conductance for $V \gg \Delta$.

For a ferromagnetic-metal/superconductor contact, the situation is somewhat different. Because the Cooper-pair is composed of a spin-up and a spin-down electron, both are required for the Andreev reflection process to take place. Consequently, when there is an imbalance in the number of spin-up and spin-down electrons at the Fermi level, as in the case of a ferromagnetic metal, the Andreev reflection probability is limited by the minority carriers in the metal. In the extreme case of $P=1$ the Andreev reflection probability is zero, because there are no spin-down states available, and thus at zero bias voltage the normalized conductance becomes $G(0)/G_n=0$. In general, for arbitrary P, it can easily be shown that

$$G(0)/G_n=2(1-P). \tag{1}$$

Equation (1) shows that a conductance measurement at small bias voltages of a metal/superconductor contact, in principle, is an experimental method to measure the spin polarization of a metal.[1–3]

It is important to recognize, however, that the simple relation of Eq. (1) is valid for a clean contact only. In real experiments, there usually will be some barrier at the metal/superconductor interface, due to oxide layers or a mismatch between the Fermi velocities of the metals. This barrier causes normal reflection of part of the current, effectively lowering the conductance, which interferes with the effects of the spin polarization. One therefore needs a model to analyze the conductance as a function of the bias voltage for nonideal contacts to reliably extract the spin polarization.

Previously, Blonder, Tinkham, and Klapwijk (BTK) have developed a theory to analyze the conductance versus bias voltage curves for *nonmagnetic*-metal/superconductor contacts.[12–14] They solved the Bogoliubov equations for a nonmagnetic-metal/superconductor interface and the effects of a barrier was included by introducing a δ-function potential at the interfaces, with dimensionless strength Z. The calculation results in a set of reflection and transmission probabilities A, B, C, and D for an incident electron with energy E. Here, A represents the Andreev reflection probability, B the probability of normal reflection, C the normal and D the Andreev transmission probability. The total current as a function of the bias voltage is found by integration of the probabilities over all energies, weighted by the Fermi-Dirac distribution function f, and reads

$$I=2e\mathcal{A}Nv_{\mathrm{F}}\int_{-\infty}^{\infty}[f(E-V,T)-f(E,T)][1+A-B]dE, \tag{2}$$

with e the electron charge, $\mathcal{A}$ the effective cross-sectional area of the contact, N the one-spin density of states at the Fermi energy and v_{F} the Fermi velocity.[12] Here, only $A=A(E,\Delta,Z)$ and $B=B(E,\Delta,Z)$ enter into Eq. (2), making use of the fact that the total probability must add up to $1(A+B+C+D=1)$. The conductance $G(V)=dI(V)/dV$ versus V curve can then be calculated at a temperature T by numerically solving and differentiating Eq. (2) as a function of the applied bias voltage V.

We have extended the model to include the spin polarization P of the metal by decomposing the current into two parts

$$I=(1-P)I_u+PI_p, \tag{3}$$

with $(1-P)I_u$ the fully unpolarized part of the current for which Andreev reflection is allowed, and PI_p the fully polarized part of the current for which the Andreev reflection probability is zero. I_u and I_p are calculated by solving Eq. (2) with the appropriate probabilities A_u, B_u, and $A_p=0$, B_p, respectively. Note that Eq. (2) shows that the current I is proportional to Nv_{F}, from which directly follows that the spin polarization measured with PCAR in the ballistic regime is $P=(N^{\uparrow}v_{\mathrm{F}}^{\uparrow}-N^{\downarrow}v_{\mathrm{F}}^{\downarrow})/(N^{\uparrow}v_{\mathrm{F}}^{\uparrow}+N^{\downarrow}v_{\mathrm{F}}^{\downarrow})$, with N^{σ} the spin-dependent density of states at the Fermi level and v_{F}^{σ} the spin-dependent Fermi velocity $(\sigma=\uparrow,\downarrow)$.

Figure 1(a) shows three normalized conductance curves, calculated using the method outlined above, for a spin polarization $P=0$, 0.35, and 1, with $Z=0$ and $\Delta=1.5$ meV. For $P=0$ the conductance is a bell-shaped curve for which $G(V)/G_n=2$ for $|V|<\Delta$ and $G(V)/G_n=1$ for $|V|\gg\Delta$. As expected, when $P=1$, $G(0)/G_n=0$, and for the intermediate case of $P=0.35$, $G(0)/G_n=2(1-P)=1.3$. Figures 1(b) and (c) show the effect of Z on the shape of the conductance curves for a spin polarization of 0.25 and 0.75, respectively. When Z increases, the Andreev reflection at low voltages is suppressed, and sharp peaks appear at Δ and $-\Delta$, characteristic for a metal/insulator/superconductor junction. Experimentally, this decrease in the Andreev reflection probability

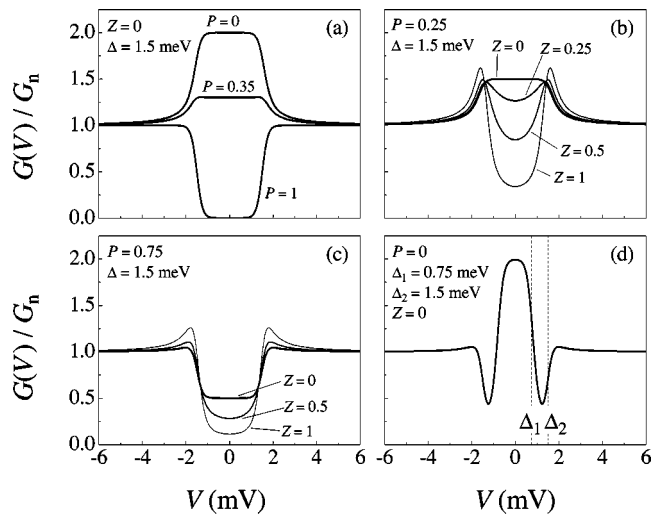

FIG. 1. Theoretical normalized conductance $G(V)/G_n$ versus V curves at $T=1.5$ K using the model described in Sec. II, with P, Z, and Δ as shown in the figure. For (a), (b), and (c) the gap value is $\Delta=\Delta_1=\Delta_2$.

should not be mistaken for substantially more spin polarization of the material under investigation. Otherwise, an exaggerated spin polarization would be concluded.

Finally, we have added one more refinement to the model. It is well known, that the Cooper pairs from a superconducting metal in close proximity to a metal can diffuse into the metal, creating a weakly superconducting layer at the metal/superconductor interface.[14,15] This superconducting proximity layer has a lower transition temperature and a lower Δ than those of the bulk. The Andreev reflection process, occurring at the metal/proximity-layer interface, is therefore limited to bias voltages smaller than the superconducting gap value of the proximity layer. However, quasiparticles can only enter the superconductor for voltages higher than the bulk gap of the Nb. This proximity effect is incorporated into our model by introducing two gap values, one for the Andreev reflection process (Δ_1), and one for the quasiparticle transport (Δ_2). Figure 1(d) shows the effect of a superconducting proximity layer on the conductance curve with $\Delta_1=0.75$ meV, $\Delta_2=1.5$ meV for a normal-metal/superconductor interface with $P=0$ and $Z=0$. Due to the proximity effect, two sharp dips appear in the conductance curve for voltages between $|\Delta_1|$ and $|\Delta_2|$.

To conclude this section we present in Table I an overview of the modified BTK Andreev- and normal-reflection probabilities, used in the calculations, for the fully unpolarized (A_u and B_u) and the fully polarized part of the current ($A_p=0$ and B_p), for energies $|E|\leqslant\Delta_1$, $\Delta_1<|E|<\Delta_2$ and $\Delta_2\leqslant|E|$.

III. EXPERIMENT

The PCAR measurements involve a small contact area because we want to measure the conductance of the metal/superconductor interface only. More specifically, the size of the contact should be of the order of or lower than the electron mean free path (Sharvin limit[16]) ensuring that the largest voltage drop occurs at the metal/superconductor interface and that we have no large resistance in series. Experimentally, PCAR measurements can be done either using a submicron pillar structure fabricated by lithography,[2] or much simpler, using a sharp tip in contact mechanically with a metal surface. The mechanical contact has the distinct advantage that many contacts can be made between the same tip and the same metal film.

The point-contact Andreev reflection measurements, described in this paper, were done using a Nb tip, pressed into the metal films by a differential screw mechanism, similar to the one described in Ref. 17. Tip and film were enclosed in a vacuum jacket immersed in a liquid helium bath. All measurements were performed at a temperature of 4.2 K. I and dI/dV versus V curves were measured using a conventional four-probe method and lock-in technique.

The Nb tip was prepared by mechanically polishing a 0.030 in. diameter Nb wire, followed by electrochemical etching in a potassium-hydroxide solution. The radius of the Nb point obtained by this method ranges between 1 and 10 μm. We have analyzed only those measurements for

TABLE I. Overview of the modified BTK Andreev- and normal-reflection probabilities for the fully unpolarized (A_u and B_u) and the fully polarized part of the current ($A_p=0$ and B_p), with $u_{01}^2=1-v_{01}^2=\frac{1}{2}\{1+[(E^2-\Delta_1^2)/E^2]^{1/2}\}$, $u_{02}^2=1-v_{02}^2=\frac{1}{2}\{1+[(E^2-\Delta_2^2)/E^2]^{1/2}\}$, $\gamma_1^2=(u_{01}^2+Z^2[u_{01}^2-v_{01}^2])^2$, $\gamma_2^2=u_{01}^2v_{01}^2+(u_{02}^2-v_{02}^2)[u_{02}^2+Z^2+(u_{02}^2-v_{02}^2)Z^2(1+Z^2)]$, and $\gamma_3^2=(u_{02}^2-v_{02}^2)[u_{02}^2+Z^2+(u_{02}^2-v_{02}^2)Z^2(1+Z^2)]$.

	Unpolarized current		Polarized current
	A_u	B_u	B_p
$\lvert E\rvert\leqslant\Delta_1$	$\dfrac{\Delta_1^2}{E^2+(\Delta_1^2-E^2)(1+2Z^2)^2}$	$1-A_u$	1
$\Delta_1<\lvert E\rvert<\Delta_2$	$\dfrac{u_{01}^2v_{01}^2}{\gamma_1^2}$	$1-A_u$	1
$\Delta_2\leqslant\lvert E\rvert$	$\dfrac{u_{01}^2v_{01}^2}{\gamma_2^2}$	$\dfrac{(u_{02}^2-v_{02}^2)^2Z^2(1+Z^2)}{\gamma_2^2}$	$\dfrac{(u_{02}^2-v_{02}^2)^2Z^2(1+Z^2)}{\gamma_3^2}$

which the contact resistance is between 1 and 100 Ω, which corresponds to an estimated contact diameter between 4 and 60 nm, within the Sharvin limit. The Ni, Co, Fe, and Cu films were prepared onto Si substrates by dc magnetron sputtering at 6 mTorr Ar pressure in a deposition chamber with a base pressure better than 1×10^{-7} Torr. The thickness of the films ranges between 2000 and 5000 Å.

IV. RESULTS AND DISCUSSION

The PCAR results in real experimental situations are rarely that of a perfectly clean contact, for which $G(0)/G_n = 2(1-P)$ applies. One needs to analyze the entire conductance curve using a model that includes the effects of a metal with spin polarization as well as the proximity effect. The experimental conductance data can be fitted to extract the spin polarization P and the barrier strength Z. Also through such analysis, one can ascertain, among many, the few conductance data with a clean contact ($Z=0$) for which the intrinsic spin polarization can be reliably determined. As illustrated below, our model provides excellent fits to the conductance data for a wide range of Z values. Most importantly, the spin polarization can be determined consistently from these results.

A. Ni, Co, and Fe

Figure 2 shows a selection of results for the PCAR measurements at $T=4.2$ K of Fe for six different contact resistances in the range between about 5 and 23 Ω. Except for Fig. 2(f), which displays the bell-shaped curve for a clean contact, the shape of the other curves is representative for a contact with a barrier at the interface, characterized by a prominent dip located at zero bias voltage due to a nonzero Z, similar to the theoretical curves shown in Fig. 1(b). All the conductance curves can be fitted very well by the model presented in Sec. II, as illustrated by the solid lines in the figure. We use only three parameters to fit the conductance curves: the spin polarization P, the interfacial scattering barrier Z, and the energy gap Δ of the superconductor. The temperature T was fixed to 4.2 K. It is assumed that $\Delta=\Delta_1=\Delta_2$, since an appreciable proximity effect is absent for Fe (and also for Co and Ni), which is due to the fact that these ferromagnetic materials act as a pair breaker for the Cooper pairs.[18] The fitted values for P, Z, and Δ are shown in the figure. Again it is clear that a detailed fit of the data is needed, because based upon the conductance at zero bias voltage alone, a significantly higher P would be concluded using Eq. (1). Note that there is no clear relationship between the contact resistance R and Z, indicating that a lower resistance does not necessarily implicate a cleaner contact. Instead, the contact resistance is largely determined by the size of the contact area. However, the fitted spin-polarization P shows a systematic variation with the barrier strength Z. Contacts with a higher Z result usually in a lower spin polarization P.

In the same manner, we have made up to 60 measurements for each Ni, Co, and Fe using several different films and Nb point contacts. All of the conductance curves can be

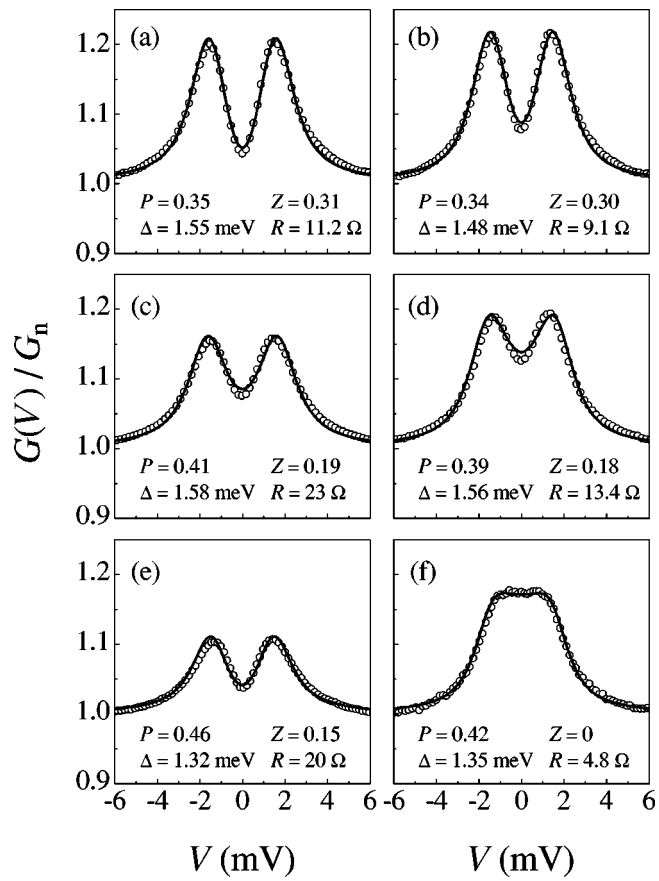

FIG. 2. Representative conductance versus voltage curves of Fe/Nb point contacts for various contact resistances R at $T=4.2$ K (open circles). The solid lines are fits using the model of Sec. II, resulting in P, Z, and Δ as indicated in the figure.

excellently fitted and the results for the spin polarization P as function of Z are shown in Fig. 3. For Ni, Co, and Fe, P decreases with increasing Z, due to negative effects of a scattering barrier at the metal/superconductor interface on the spin polarization. Formation of metal oxides and metal/Nb alloying at the interface cause spin-mixing effects and dilute the intrinsic polarization of the bulk material. The scatter in the values of P at high Z is probably related to the specific composition of the barrier and its influence on P. Most importantly, the intrinsic spin polarization of the current can be reliably extracted in the limit of $Z=0$, as is demonstrated by the parabolic fit of the data shown by the solid line in Fig. 3, resulting in $P=0.37\pm0.01$, 0.45 ± 0.02, and 0.43 ± 0.03 for Ni, Co, and Fe, respectively.

The values for the spin polarization of Co and Fe can be compared with those recently obtained using high quality superconducting tunnel junctions. The values of $P=0.42$ and 0.45 for Co and Fe, respectively, as reported by Monsma *et al.*,[9] agree very well with our results. In the same study, on the other hand, a considerably lower spin polarization $P=0.29$ was found for Ni. However, Ni-alumina alloy formation is problematic in these tunnel junctions, which considerably reduces the apparent spin polarization of Ni obtained by this method.[19]

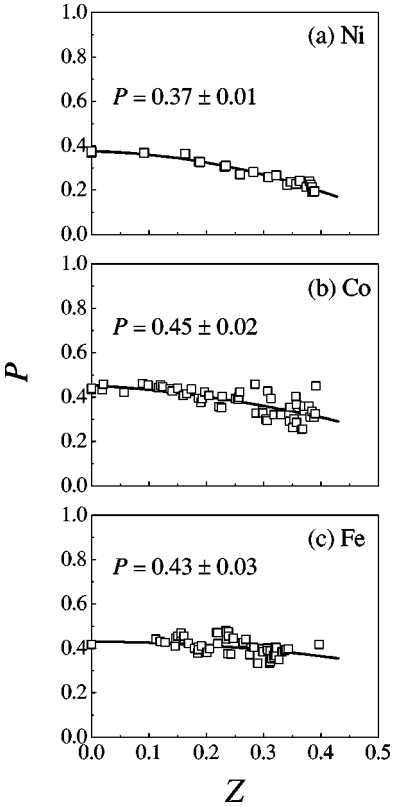

FIG. 3. Fitted spin polarization P as function of Z at $T=4.2$ K for (a) Ni, (b) Co, and (c) Fe. The solid line is a parabolic fit of the data to extract P in the limit of $Z=0$.

B. Cu

In a similar manner as for the magnetic materials described above, we have measured about 35 conductance-voltage curves for a Nb point contact on Cu. Figures 4(a) and (b) show two representative normalized conductance versus voltage curves with a contact resistance of 7.6 and 2.4 Ω, respectively. For both curves $G(0)/G_n$ is not 2, due to a nonzero Z and the effects of a finite measuring temperature. There is a pronounced proximity effect in the Cu, characterized by the two dips in the conductance between $|\Delta_1|$ and

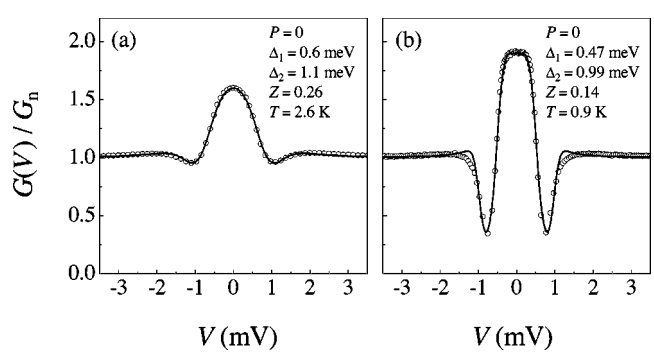

FIG. 4. Representative conductance versus voltage curves for Cu/Nb at $T=4.2$ K (open circles) with a contact resistance of (a) $R=7.6$ Ω and (b) $R=2.4$ Ω. The solid lines are fits using the model of Sec. II, resulting in P, Δ_1, Δ_2, Z, and T as indicated in the figure.

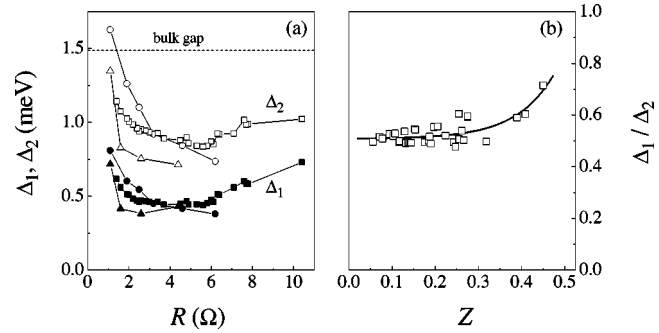

FIG. 5. (a) Evolution of the superconducting gap values Δ_1 (solid symbols) and Δ_2 (open symbols) as function of the contact resistance for three different series of measurements using different Cu films and Nb point contacts. (b) Ratio Δ_1/Δ_2 as function of Z (open squares). The solid line is a guide to the eye.

$|\Delta_2|$ at positive and negative bias voltages, similar to the theoretical curve of Fig. 1(d). The proximity effect is more pronounced for a clean contact with a low Z.

The solid curves are fits to the data with the model of Sec. II using two gap values, which resulted in values for P, Δ_1, Δ_2, Z, and T as shown in the figure. We want to emphasize that as expected for nonmagnetic Cu, the extracted spin polarization P, despite very substantial Z is consistently 0. The two dips in the conductance curves are very deep and have sharp edges. This is surprising because of the considerable thermal broadening that is expected at 4.2 K. Apparently there are nonequilibrium transport processes present when the proximity effect in the Cu plays an important role. Since temperature is included in our model by an equilibrium Fermi-Dirac distribution function, the fitted temperature is considerably lower than 4.2 K, as shown in Fig. 4. Formally including nonequilibrium processes in the calculations, however, would require an entirely different approach, which is beyond the scope of this paper.[20,21] Nevertheless, apart from this discrepancy there is an overall excellent agreement between experimental and fitted conductance-voltage curves.

Figure 5(a) shows the evolution of the fitted gap values Δ_1 and Δ_2 as a function of the contact resistance between 1.1 and 10.1 Ω for three series of Cu/Nb PCAR measurements using different films and Nb point contacts. Although there is some difference in the absolute values between the different measurements, the three films show basically the same behavior. Going from small to larger contact resistance, that is going from a large to a small contact area, both Δ_1 and Δ_2 first display a sharp decrease and then a slight increase. We attribute the initial decrease to the fact that, when the size of the contact approaches the superconducting coherence length ξ_{Nb}, the superconductivity in the end of the Nb tip is suppressed. We have estimated that at a contact resistance of approximately 3 Ω, the diameter of the contact area becomes equal to the coherence length $\xi_{Nb}=38$ nm.[22] For higher contact resistances a slight increase of Δ_1 and Δ_2 is observed. These high resistance contacts are usually accompanied by a large Z, which leads to the somewhat higher gap values because of a reduced proximity effect.

Although the overall values of Δ_1 and Δ_2 show a large variation for different measurements depending on the con-

tact resistance, the ratio of Δ_1/Δ_2 is surprisingly constant. Figure 5(b) shows Δ_1/Δ_2 as function of Z for all Cu/Nb PCAR measurements. The ratio Δ_1/Δ_2 approaches 0.5 in the limit of a clean contact, when the proximity effect is most pronounced. The reason for this factor 0.5 needs further theoretical examination. One could argue that this factor represents the average gap value for the superconducting proximity layer in the Cu, which is roughly half that of the bulk gap value.

V. CONCLUSIONS

In conclusion, we have analyzed the PCAR measurements of X/Nb, with $X=$Ni, Co, Fe, and Cu. Experimental conductance-voltage curves were analyzed with the BTK theory, modified to include the spin polarization of the current P and superconducting proximity effects in the metal. The polarization for Fe, Co, and Ni depends substantially on the quality of the metal/superconductor contact. The value of the intrinsic spin polarization of the current can be obtained by extrapolation to $Z=0$ (perfectly transparent interface), resulting in $P=0.37\pm0.01$, 0.45 ± 0.02, and 0.43 ± 0.03 for Ni, Co, and Fe, respectively. For Cu, the conductance-voltage curves show a dip at the position of the Nb superconducting gap. This dip can be attributed to a weakly superconducting layer in the Cu at the Cu/Nb interface, which reduces the effective gap value for the Andreev reflection process, while leaving the gap for quasiparticle transport essentially unchanged. In addition, an overall decrease of the gap is observed when the size of the point contact approaches the superconducting coherence length in Nb.

ACKNOWLEDGMENTS

This work was supported by NSF Grant Nos. DMR96-32526 and DMR97-32763.

[1] M.J.M. de Jong and C.W.J. Beenakker, Phys. Rev. Lett. **74**, 1657 (1995).
[2] S.K. Upadhyay, A. Palanisami, R.N. Louie, and R.A. Buhrman, Phys. Rev. Lett. **81**, 3247 (1998).
[3] R.J. Soulen, J.M. Byers, M.S. Osofsky, B. Nadgorny, T. Ambrose, S.F. Cheng, P.R. Broussard, C.T. Tanaka, J. Nowak, J.S. Moodera, A. Barry, and J.M.D. Coey, Science **282**, 85 (1998).
[4] G. Prinz, Phys. Today **48**(4), 58 (1995).
[5] J.M. Daughton, A.V. Pohm, R.T. Fayfield, and C.H. Smith, J. Phys. D **32**, R169 (1999).
[6] I.I. Mazin, Phys. Rev. Lett. **83**, 1427 (1999).
[7] R. Meservey and P.M. Tedrow, Phys. Rep. **238**, 173 (1994).
[8] R.J.M. van de Veerdonk, J.S. Moodera, and W.J.M. de Jonge (unpublished).
[9] D.J. Monsma and S.S.P. Parkin, Appl. Phys. Lett. **77**, 720 (2000).
[10] P. LeClair, H.J.M. Swagten, J.T. Kohlhepp, R.J.M. van de Veerdonk, and W.J.M. de Jonge, Phys. Rev. Lett. **84**, 2933 (2000).
[11] A.F. Andreev, Zh. Éksp. Teor. Fiz. **46**, 1823 (1964) [Sov. Phys. JETP **19**, 1228 (1964)].
[12] G.E. Blonder, M. Tinkham, and T.M. Klapwijk, Phys. Rev. B **25**, 4515 (1982).
[13] G.E. Blonder and M. Tinkham, Phys. Rev. B **27**, 112 (1983).
[14] M. Tinkham, *Introduction to Superconductivity* (McGraw-Hill, Inc., New York, 1996).
[15] C.L. Chien and D.H. Reich, J. Magn. Magn. Mater. **200**, 83 (1999).
[16] Y.V. Sharvin, Zh. Éksp. Teor. Fiz. **48**, 984 (1965) [Sov. Phys. JETP **21**, 655 (1965)].
[17] A.G.M. Jansen, A.P. van Gelder, and P. Wyder, J. Phys. C **13**, 6073 (1980).
[18] J.J. Hauser, H.C. Theuerer, and N.R. Werthamer, Phys. Rev. **142**, 118 (1966).
[19] D.J. Monsma and S.S.P. Parkin, Appl. Phys. Lett. **77**, 883 (2000).
[20] A. Martin and C.J. Lambert, Phys. Rev. B **51**, 17 999 (1995).
[21] J. Sánchez-Cañizares and F. Sols, Phys. Rev. B **55**, 531 (1997).
[22] C. Kittel, *Introduction to Solid State Physics*, 6th ed. (John Wiley & Sons, Inc., New York, 1986).